J. theor. Biol. (2002) **214,** 577–597
doi:10.1006/jtbi.2001.2476, available online at http://www.idealibrary.com on IDEAL®

A Model for the Enhancement of Fitness in Cyanobacteria Based on Resonance of a Circadian Oscillator with the External Light–Dark Cycle

DIDIER GONZE*, MARC R. ROUSSEL† AND ALBERT GOLDBETER*‡

**Unité de Chronobiologie théorique, Faculté des Sciences, Université Libre de Bruxelles, Campus Plaine, C.P. 231, B-1050 Brussels, Belgium and †Department of Chemistry and Biochemistry, University of Lethbridge, Alberta, T1K 3M4 Canada*

(*Received on* 27 *June* 2001, *Accepted in revised form on* 17 *October* 2001)

Fitness enhancement based on resonating circadian clocks has recently been demonstrated in cyanobacteria [Ouyang *et al.* (1998). *Proc. Natl Acad. Sci. U.S.A.* **95,** 8660–8664]. Thus, the competition between two cyanobacterial strains differing by the free-running period (FRP) of their circadian oscillations leads to the dominance of one or the other of the two strains, depending on the period of the external light–dark (LD) cycle. The successful strain is generally that which has an FRP closest to the period of the LD cycle. Of key importance for the resonance phenomenon are observations which indicate that the phase angle between the circadian oscillator and the LD cycle depends both on the latter cycle's length and on the FRP. We account for these experimental observations by means of a theoretical model which takes into account (i) cell growth, (ii) secretion of a putative cell growth inhibitor, and (iii) the existence of a cellular, light-sensitive circadian oscillator controlling growth as well as inhibitor secretion. Building on a previous analysis in which the phase angle was considered as a freely adjustable parameter [Roussel *et al.* (2000). *J. theor. Biol.* **205,** 321–340], we incorporate into the model a light-sensitive version of the van der Pol oscillator to represent explicitly the cellular circadian oscillator. In this way, the model automatically generates a phase angle between the circadian oscillator and the LD cycle which depends on the characteristic FRP of the strain and varies continuously with the period of the LD cycle. The model provides an explanation for the results of competition experiments between strains of different FRPs subjected to entrainment by LD cycles of different periods. The model further shows how the dominance of one strain over another in LD cycles can be reconciled with the observation that two strains characterized by different FRPs nevertheless display the same growth kinetics in continuous light or in LD cycles when present alone in the medium. Theoretical predictions are made as to how the outcome of competition depends on the initial proportions and on the FRPs of the different strains. We also determine the effect of the photoperiod and extend the analysis to the case of a competition between three cyanobacterial strains.

1. Introduction

Among oscillatory processes in biological systems, circadian rhythms are conspicuous by their ubiquity. These rhythms, of a period close to 24 hr, indeed occur in nearly all living organisms, from multicellular to unicellular, including some bacterial species (Edmunds, 1988; Wilsbacher & Takahashi, 1998; Dunlap, 1999). The major role generally ascribed to circadian rhythms is to allow living organisms to anticipate the daily alternation of light and darkness and to adapt to

‡Author to whom correspondence should be addressed. E-mail: agoldbet@ulb.ac.be

0022–5193/02/040577 + 21 $35.00/0

the periodic variation of the environment. The effects of light–dark (LD) cycles on longevity have mainly been studied in *Drosophila* where early investigations showed that flies live longer in 24-hr LD cycles than in LD cycles of smaller or longer period [Pittendrigh & Minis, 1972; see Klarsfeld & Rouyer (1998) for a reexamination of this issue]. Furthermore, the lifespan of flies was significantly reduced in continuous light compared to continuous darkness or LD cycles (Allemand *et al*., 1973; Sheeba *et al*., 2000).

The best demonstration of the adaptive role of circadian rhythms is provided by recent experiments carried out by Ouyang *et al.* (1998) in *Synechococcus*, a cyanobacterium. These experiments have shown the existence of a resonance phenomenon enhancing fitness in these bacteria, for which circadian rhythms have been characterized in recent years (Huang *et al*., 1990; Kondo *et al*., 1993, 1994; Liu *et al*., 1995; Johnson *et al*., 1996, 1998; Golden *et al*., 1998; Kondo & Ishiura, 1999). Thus, when the wild type, which has a free-running period close to 25 hr in continuous light, is mixed with a mutant strain characterized by a free-running period (FRP) of 22 or 30 hr, the outcome of the competition between the two strains depends on the relative closeness of the free-running periods with the period of the imposed light–dark (LD) cycle. The strain that wins the competition is generally that whose FRP is closest from the period of the LD cycle. This difference in fitness occurs despite the fact that the wild-type and mutant strains possess identical growth characteristics when cultured alone. While the mechanism underlying this resonance effect is still not characterized at the molecular level, the experiments have shown that the phase angle between the cell circadian oscillator and the external LD cycle depends on the FRP of each strain and therefore differs for the mutants and for the wild type; moreover, this phase angle varies with the period of the external LD cycle.

We have recently developed a theoretical approach (Roussel *et al*., 2000) to account for the observations of Ouyang *et al.* (1998) on the outcome of competition experiments between wild-type and clock mutant strains of cyanobacteria subjected to LD cycles of various periods. This first approach compared two possible mechanisms capable of giving rise to fitness differences according to the phase angle of the competing strains with respect to the external LD cycle. This study showed that the most likely mechanism rests on the secretion of a growth inhibitor by the cyanobacterial strains, when both secretion and sensitivity toward the inhibitor depend on the phase of the circadian oscillator and of the LD cycle. While such a mechanism could successfully account for experimental observations in LD and LL (continuous light) conditions, a mechanism based on competition of the wild-type and mutant strains for a common substrate only led to such agreement in LD conditions but could not apply to LL conditions.

The theoretical model that we previously proposed (Roussel *et al*., 2000) rests on the existence of a phase angle between the circadian oscillator and the LD cycle. In this model the light-sensitive circadian oscillator was not represented explicitly by a continuous oscillator; the phase angle θ was simply defined as the phase difference between the onset of the subjective light phase (sL) and the beginning of the L phase of the external LD cycle. The underlying idea was that there exists some functional relationship between θ, the LD cycle length, and the strain-dependent FRP. However, we advanced no particular hypothesis on the form of this relationship, other than that we expect smaller phase angles to be observed when the LD cycle length and FRP are similar. The phase angle was thus considered as a parameter expressed as a fraction of the external LD cycle, varying from -0.5 (phase delay) to $+0.5$ (phase advance). It would be more satisfactory if the phase angle, rather than being considered as a parameter whose value is arbitrarily set, would emerge from the model itself. To this end, here we represent the circadian rhythm explicitly by a continuous, light-sensitive oscillator of the limit cycle type. We resort to a version of the van der Pol oscillator, which has long been used for modeling various properties of circadian rhythms, such as the phase-shifting effect of external perturbation by light pulses (Kronauer *et al*., 1997; Jewett & Kronauer, 1998; Jewett *et al*., 1999). The value of the phase angle θ then naturally originates from the periodic forcing of the cellular (van der Pol) oscillator by the external LD cycle.

In Section 2, we present the model and the hypotheses underlying the effect of light on the cellular circadian oscillator, cell growth and inhibitor secretion. In Section 3.1, we show how the phase angle varies as a function of the period of the external LD cycle. Growth of individual strains in LL or LD is considered in Section 3.2. In Section 3.3, we turn to the competition between wild-type and clock mutant strains in LD cycles of various periods. We focus, in particular, on the effect of initial conditions, of the inhibition threshold, and of the photoperiod on the outcome of competition experiments. In Section 3.4, we extend these results to the case of competition involving three bacterial strains of different FRP. In the last section, we discuss these results and show that the model gives a mechanism accounting for all available experimental observations, both for LL and LD conditions, for individual or mixed cultures, in terms of a continuous, light-sensitive cellular oscillator of the limit cycle type. The model provides a unified framework for the various experimental findings, and explains how resonating circadian clocks enhance fitness in cyanobacteria. It allows the rapid study of a large variety of experimental conditions and thereby leads to a number of testable predictions.

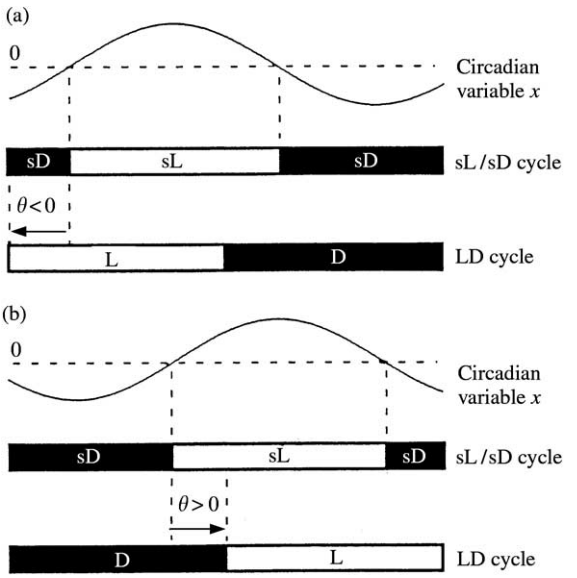

FIG. 1. Phase angle between the circadian oscillator and the light–dark (LD) cycle. The subjective day (sL phase) corresponds to the phase during which the circadian variable x (whose time course is generated by the van der Pol oscillator model) takes positive values; subjective night (sD) corresponds to negative values of x. The phase angle θ is defined as the phase difference, expressed as a fraction of the LD cycle, between the onset of sL and the beginning of L. Thus $\theta < 0$ corresponds to a delay of sL with respect to L (panel a), while $\theta > 0$ corresponds to an advance of sL with respect to L (panel b).

2. Model Based on Resonance of a Circadian Oscillator with the External Light–Dark Cycle

The model is presented in three stages. First we introduce the definition of the phase angle between the circadian oscillator and the external LD cycle. Second, we specify how the inhibitor affects growth, as well as the manner in which growth and inhibitor secretion depend on light. We present the equations governing cell growth as a function of inhibitor and light. Lastly, we introduce the equations governing the cell circadian rhythm in the form of a modified version of the van der Pol oscillator.

2.1. DEFINITION OF PHASE ANGLE θ

We start by defining, as in our previous publication, the phase angle θ that separates the cell circadian oscillator (to be defined below in an explicit manner) and the external LD cycle. We assume (see Fig. 1) that the circadian rhythm occurs in a variable x, such that when x exceeds a threshold—arbitrarily set equal to zero—the organism is in subjective day (sL). Conversely, when $x < 0$, the organism is in subjective night (sD). The sL and sD phases correspond to different metabolic states, both with respect to inhibitor production and sensitivity of growth toward the inhibitor (see below).

The phase angle θ is defined as the phase difference between the onset of the sL phase and the beginning of the L phase of the external LD cycle. By definition, $\theta < 0$ corresponds to a phase delay of sL with respect to L [Fig. 1(a)], while $\theta > 0$ corresponds to a phase advance [Fig. 1(b)].

The phase angle is measured as a fraction varying between -0.5 and $+0.5$. When $\theta = 0$, sL and L start concomitantly; when sL is delayed with respect to L, the value of θ is negative and progressively goes from 0 to -0.5 as the beginning of sL approaches the beginning of D [Fig. 1(a)]. When this occurs, as soon as the onset

of sL starts after the beginning of D, the value of θ becomes positive and progressively goes from $+0.5$ to 0 as the onset of sL approaches the beginning of L [Fig. 1(b)].

2.2. DEPENDENCE OF CELL GROWTH ON THE PHASE OF CIRCADIAN OSCILLATIONS

If a competition between two different strains of the same cyanobacterial species exists, this implies that the two strains either compete for nutrient resources, or that they mutually hinder each other by producing some inhibitor to which they are sensitive only during part of their sL/sD cycle. Our previous theoretical study showed that the latter hypothesis is more likely to hold, as it applies to LD as well as LL conditions, in contrast to the former assumption which only applies to LD but is impossible to reconcile with experimental observations in LL. Therefore, we will focus here on the mechanism of competition involving the production of a growth inhibitor rather than competition based on substrate depletion.

As in our previous, more abstract model, we assume that cells produce the inhibitor only during their sL phase, and that growth occurs only in L (Fig. 2). When sL overlaps with L, growth occurs unconditionally, i.e. cells are insensitive to the inhibitor. When sD overlaps with L, growth occurs if the level I of inhibitor is below a threshold value I_c. We further assume that inhibitor degradation takes place all the time.

The equations governing the time evolution of cell population N_i ($i = 1, \ldots, n$) and the level of inhibitor I are given below:

$$\frac{\mathrm{d}N_i}{\mathrm{d}t} = k_i N_i \left(1 - \sum_{j=1}^{n} N_j\right) - \gamma N_i,$$

$$\frac{\mathrm{d}I}{\mathrm{d}t} = \sum_{i=1}^{n} N_i \left(p_i - \frac{V_{max} I}{K_M + I}\right) - \gamma I \qquad (1)$$

with:

$$k_i = \begin{cases} k & \text{in L and strain } i \text{ is in sL or } I < I_c, \\ 0 & \text{otherwise,} \end{cases}$$

$$p_i = \begin{cases} p & \text{when strain } i \text{ is in sL,} \\ 0 & \text{otherwise.} \end{cases} \qquad (2)$$

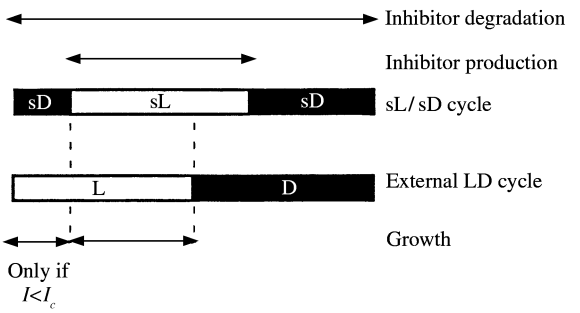

FIG. 2. Hypotheses underlying the model for competition based on resonating circadian clocks. Cells are assumed to grow when their subjective phase sL overlaps with L; growth also occurs when their sD phase overlaps with L, but only if the inhibitor level is below a threshold I_c. The inhibitor is secreted by cells during sL and degraded continuously, throughout sL and sD.

In these equations, N_i denotes the number of (synchronized) cells of strain i, and I represents the inhibitor concentration; parameter k measures the growth rate of each bacterial strain; parameter γ is a dilution factor; p measures the rate of inhibitor production; V_{max} and K_M represent, respectively, the maximum rate and the Michaelis constant characterizing the enzymatic degradation of the inhibitor. In agreement with experimental observations, all bacterial strains are characterized by the same growth rate in monoculture. Likewise we assume that all strains produce the inhibitor at the same rate. We will only consider the case of batch cultures ($\gamma = 0$) with occasional dilutions of the medium.

We have verified that similar results are obtained when replacing the all-or-none dependence of parameter k on I in eqns (2) by a continuous dependence described by a Hill function. Simulations indicate that when the dependence of k on I has a continuous sigmoidal shape, the variations of I are so rapid with respect to the circadian time-scale that the changes in k acquire a quasi-all-or-none nature.

The circadian oscillator variable x appears in the above equations through the definition of phase sL in eqns (2): this phase corresponds to values $x > 0$. The above equations are the same as those considered in our previous theoretical study of the resonance phenomenon. In contrast to our previous work, however, we will incorporate an explicit mechanism producing sustained oscillations in x. This mechanism, which is sensitive to light, allows entrainment of the circadian

oscillator by the external LD cycle and automatically produces a phase angle between these two rhythms.

2.3. MODELING THE CELL CIRCADIAN RHYTHM BY A LIMIT CYCLE OSCILLATOR

As explained above, the major difference between the present model and our previous effort pertains to the incorporation of a mechanism producing sustained circadian oscillations in the cellular variable x. We could have used a molecular model for circadian oscillations, such as those proposed for *Drosophila* or for *Neurospora* (Leloup & Goldbeter, 1998, 2000; Leloup *et al*., 1999; Gonze *et al*., 2000). However, the detailed molecular mechanism of circadian rhythmicity in *Synechococcus* remains unclear, even if some clock genes—notably *kaiA*, *kaiB* and *kaiC*—have already been identified in this organism (Ishiura *et al*., 1998; Kondo & Ishiura, 1999). The alternative, which we have adopted, is to resort to a mathematical model extensively used for simulating properties of circadian oscillations, but unrelated to any specific molecular mechanism. The van der Pol equations were originally proposed to describe sustained oscillations in electrical circuits and have been used in modeling circadian oscillations for over three decades. Of particular relevance to our study is the use of the van der Pol oscillator to account for phase shifts of circadian rhythms by light pulses.

We shall use a modified version of the van der Pol oscillator recently introduced by Jewett & Kronauer (1998; see also Kronauer *et al*., 1997) in a study of the effect of light on human circadian rhythms. The phenomenological equations proposed in the form of eqns (3) produce sustained oscillations of the limit cycle type in variable x, with a circadian free-running period (in LL) close to τ_x; x_c represents a second, complementary variable, and $B(t)$ is a light-controlled parameter which depends on light intensity ρ. In the paper by Jewett and Kronauer, the expression for parameter B is slightly different and light intensity is denoted by I, a symbol which we reserve for the inhibitor concentration.

$$\frac{dx}{dt} = 24\frac{\pi}{12}\left(x_c + 0.13\left(\frac{x}{3} + \frac{4}{3}x^3 - \frac{256}{105}x^7\right) + B(t)\right),$$

$$\frac{dx_c}{dt} = 24\frac{\pi}{12}\left(-x\left(\frac{24}{\tau_x}\right)^2 + \frac{B(t)}{3}x_c - 0.15B(t)x\right) \tag{3}$$

with

$$B(t) = \left(1 - \frac{x}{3}\right)0.39\,\rho^{0.23},$$

$$\rho = \begin{cases} 5 & \text{in light phase (L),} \\ 0 & \text{in dark phase (D).} \end{cases}$$

The coupling between the external LD cycle and the circadian oscillator is thus introduced via parameter B. This parameter depends on the light intensity ρ which goes from zero in the D phase up to a constant, non-vanishing value (equal to 5 in the simulations) during the L phase. Sustained oscillations in variable x with a period of the order of 25 hr as in the wild-type *Synechococcus*, or 30 hr as in a mutant cyanobacterial strain are readily obtained by setting parameter τ_x equal to 25 or 30, respectively.

3. Results

3.1. THE PHASE ANGLE VARIES AS A FUNCTION OF THE PERIOD OF THE EXTERNAL LD CYCLE

In the following, we will illustrate the behavior of the model mainly by considering the wild-type ($\tau = 25$ hr) and a long-period mutant ($\tau = 30$ hr). For the sake of clarity, in most figures we will not consider other cases, such as that of a short-period mutant, but the model can readily be applied to any FRP. Moreover, the role of the FRP on the outcome of competition experiments will be considered in detail in Section 3.3 below.

We first show in Fig. 3 (first row) that the model governed by eqns (3) can produce sustained oscillations of variable x in continuous light, i.e. LL conditions. The upper left panel in Fig. 3 corresponds to the circadian oscillatory behavior of wild-type *Synechococcus* cyanobacteria, with an FRP close to 25 hr, while the upper right panel shows the behavior of a long-period clock mutant whose FRP is close to 30 hr. The middle and bottom rows in Fig. 3 illustrate the entrainment of the circadian oscillator model by a 12:12 LD cycle and a 15:15 LD cycle, respectively (the case of unequal durations of the L and

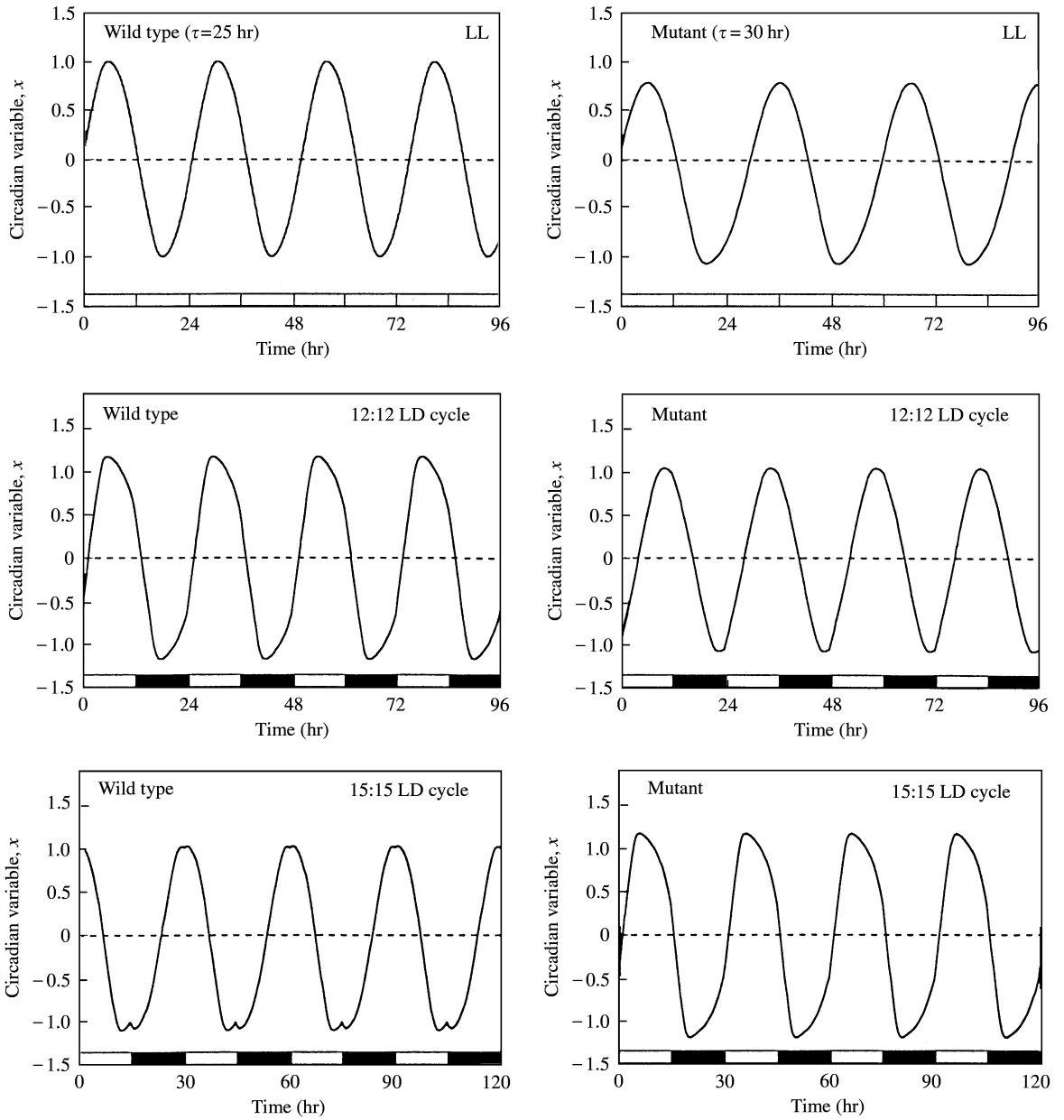

FIG. 3. Circadian oscillations produced by the modified van der Pol model in LL (upper row) and in a 12:12 (middle row) and 15:15 (bottom row) LD cycle, corresponding to the wild-type ($\tau = 25$ hr; left column) and the long-period mutant ($\tau = 30$ hr; right column) strains of cyanobacteria. The evolution of variable x, determined by numerical integration of eqns (3), is shown as a function of time. Parameter values (used throughout this study) are $\rho = 5$ in LL; in LD, $\rho = 5$ in L and 0 in D. Parameter τ_x in eqns (3), which is very close to the free-running period τ, is equal to 25 and 30 hr for the left and right columns, respectively. Of importance for the competition process is the fact that the sL phase ($x > 0$) largely overlaps with the L phase when the wild-type strain ($\tau = 25$ hr) is placed in a 12:12 LD cycle (middle left panel) and when the long-period mutant ($\tau = 30$ hr) is placed in a 15:15 LD cycle. Moreover, the sL phase is delayed with respect to L in the long-period mutant in a 12:12 LD cycle (middle right panel) while sL is advanced with respect to L in the wild type in a 15:15 LD cycle (left bottom panel).

D phases will be considered in Section 3.3). As explained above, the entrainment is achieved by periodically changing the light intensity ρ which controls parameter B in eqns (3).

Besides demonstrating that the modified van der Pol oscillator model can oscillate autonomously with a circadian period in LL and can entrain to LD cycles of various periods, the data

of Fig. 3 show that, in agreement with experimental observations, the phase angle between the cellular circadian oscillator and the external LD cycle changes with the period of the LD cycle and is characteristic of each strain, i.e. it also depends on the FRP (τ).

A comparison of the middle and bottom rows in Fig. 3 indicates that when the FRP is close to the period of the LD cycle, then the time at which x becomes positive (which corresponds to the beginning of the sL phase) roughly corresponds to the beginning of the L phase: this is observed for the wild type ($\tau = 25$ hr) in the 12:12 LD cycle, and for the mutant ($\tau = 30$ hr) in the 15:15 LD cycle. Moreover, when the period of the LD cycle is larger than the FRP, the sL phase is advanced with respect to the L phase (see lower left panel for the wild type in 15:15 LD). Conversely, when the period of the LD cycle is smaller than the FRP, the sL phase is delayed with respect to the L phase (see middle right panel for the 30-hr-period mutant in 12:12 LD). These differences, which agree well with the observations of Ouyang *et al.* (1998) (see their Fig. 4), underlie the resonance effect described by these authors and analysed below by means of the model.

The dependence of the phase angle θ in the wild type and in the 30-hr-period mutant on the forcing period T (i.e. the period of the external LD cycle) over a wide range extending from 22 to 30 hr is shown in Fig. 4(a). Below and above this range, complex oscillatory behavior in the form of quasi-periodic oscillations is observed instead of simple entrainment (such behavior can already be seen for the mutant for $T < 22.4$ hr). We will focus in the following on the range of forcing periods yielding simple entrainment, not only because the interpretation of the results is more straightforward, but also because the experiments have been carried out under such conditions.

The results shown in Fig. 4(a) corroborate the above conclusion as to the occurrence of a delay of sL with respect to L ($\theta < 0$) when T is roughly below the FRP, and of an advance of sL with respect to L ($\theta > 0$) when T is roughly above the FRP. For the long-period mutant, because the forcing period is below the FRP in most of the range considered in Fig. 4, the value of θ for

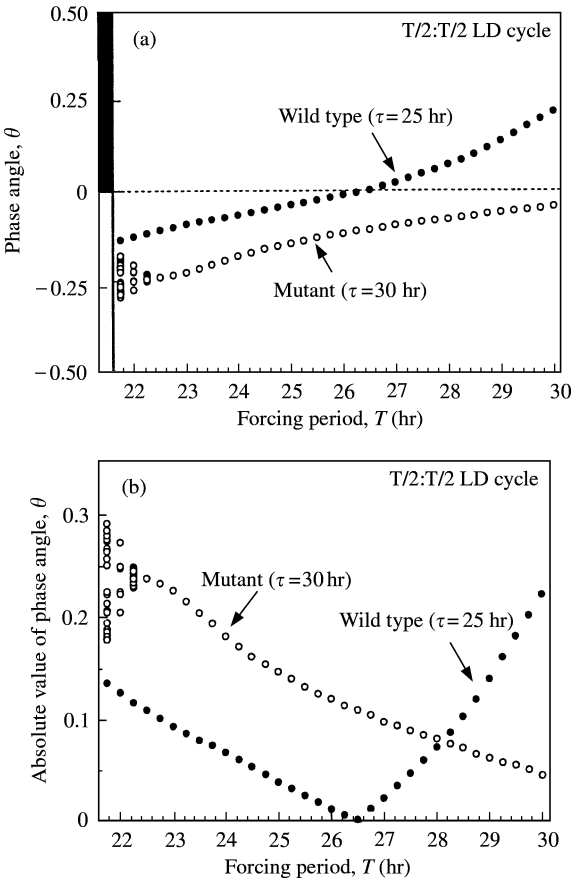

FIG. 4. Phase angle as a function of period T of external LD cycle in the wild-type and long-period mutant strains. In the range of forcing period considered, which extends from 22 to 30 hr, the phase angle, which differs for the two strains, goes from a negative value (sL delayed with respect to L) to a positive value (sL advanced with respect to L) for the wild-type strain, and remains negative for the long-period strain [panel (a)]. The phase angle, defined in Fig. 2, ranges from -0.5 (sL begins near the end of L) to $+0.5$ (sL begins near the beginning of D). The data of panel (a) are replotted in absolute value in panel (b). The LD cycle considered is symmetrical, i.e. the L and D phase have similar durations equal to $T/2$. For the long-period mutant, the phase is labile at small values of T but nevertheless remains confined in a narrow range of phases. The two curves in panel (b) intersect near $T = 28$ hr. This value separates LD cycles in which the wild-type or the long-period mutant strain becomes dominant (see Fig. 6).

this mutant remains negative so that the sL phase is always delayed with respect to L. In contrast, for the wild type, the FRP falls within the range of forcing periods considered so that the phase angle θ goes from a negative to a positive value as T increases, and the delay of sL with respect to L transforms into an advance.

Also important for the following part of this paper is the observation that at low values of the

forcing period, the phase angles of the wild-type and of the long-period mutant are both negative in Fig. 4(a) (in both strains sL is delayed with respect to L), while at large values of T the phase angles of these two strains have opposite signs (sL is advanced with respect to L in the wild type, and delayed in the mutant).

We will see that with regard to the resonance effect, the absolute magnitude of the phase angle θ is crucial for the outcome of competition between strains with different FRPs. Indeed, it is when the absolute value of the phase angle is small that the overlap of sL with L is significant; at that time cells secrete the inhibitor but are insensitive to it and grow, while retaining the capability of hampering the growth of other strains characterized by a different phase angle. It is therefore useful to replot the results of Fig. 4(a) by showing the absolute value of θ as a function of the forcing period T. This is done in Fig. 4(b) for the same two strains considered in Fig. 4(a). Below a value of T close to 28 hr, the absolute value of the wild-type phase angle is shorter than that of the long-period mutant, and the contrary situation occurs above this T value.

3.2. GROWTH OF INDIVIDUAL STRAINS IN LL OR LD

A major constraint on the model is set by experiments which indicate that when various strains of cyanobacteria differing by their FRP are placed alone in the cell culture, they all display the same growth kinetics in LL and in LD cycles, regardless of the LD period. This is in part due to the identity of the kinetic parameters (k, p, V_{max} and K_M) for all strains in our model. However, this property of the model also depends somewhat on the values of the kinetic parameters, and particularly on the inhibitor clearance kinetics.

Simulations of the growth of cultures containing only the wild-type or the long-period mutant strain in LL conditions are shown in Fig. 5(a). The curves for the two strains are quasi-identical, in agreement with experimental observations. The reason as to why the two strains grow in a similar manner stems from the fact that in both cases, cells grow nearly all the time, both in sL and in sD (because they experience continuous illumination), except at the transition between sL and sD where the level of inhibitor prevents growth during the period necessary to bring I below the inhibitory threshold I_c. If the degradation is rapid, as in the case of Fig. 5(a), this time will be so short that the arrest of growth will be unnoticeable. However, the model in LL can generate slightly distinct curves for cyanobacterial strains possessing different FRPs at lower values of the maximum rate of inhibitor degradation. In such a case, illustrated in Fig. 5(d), there is a slight arrest of growth for each strain just after the transition from sL to sD. Because the durations of the sL and sD phases vary for different strains, these brief plateaus—which have been observed experimentally and are referred to as "circadian gating" (Mori *et al.*, 1996)—will not occur at the same time for each strain. As a result, the growth curves will not be as close to each other as in the case of Fig. 5(a), but they nevertheless remain very close.

Differences between the growth curves in LD can be more significant than in LL, but again this depends on the maximum rate of inhibitor degradation. When this rate is large, the growth curves for cultures containing solely the wild-type or the long-period mutant are quasi-identical, as illustrated in Fig. 5(b) and (c) for the cases of a 12 : 12 and a 15 : 15 LD cycle, respectively. This is due to the fact that each culture grows during an equal time (the full duration of the L phase), regardless of its FRP. Indeed, at the end of sL, if the beginning of sD falls in L, the level of I is rapidly brought below the threshold I_c so that growth is practically uninterrupted.

Differences in growth kinetics may occur in LD at lower values of the maximum rate of inhibitor degradation. The differences remain small in a 12 : 12 LD cycle [Fig. 5(e)] but are maximized when forcing the culture by LD cycles of longer period, e.g. 30 hr [Fig. 5(f)], particularly when the two strains compared have phase angles of opposite signs. For example, as shown in Fig. 4(a), when forcing by a 30-hr LD cycle, the wild-type strain ($\tau = 25$ hr) has a positive phase angle—i.e. the beginning of sD falls in L—while the long-period mutant ($\tau = 30$ hr) has a negative θ—the beginning of sD falls in D. When the beginning of sD falls in D, growth does not occur after the sL to sD transition. The next growth phase will begin as soon as the next

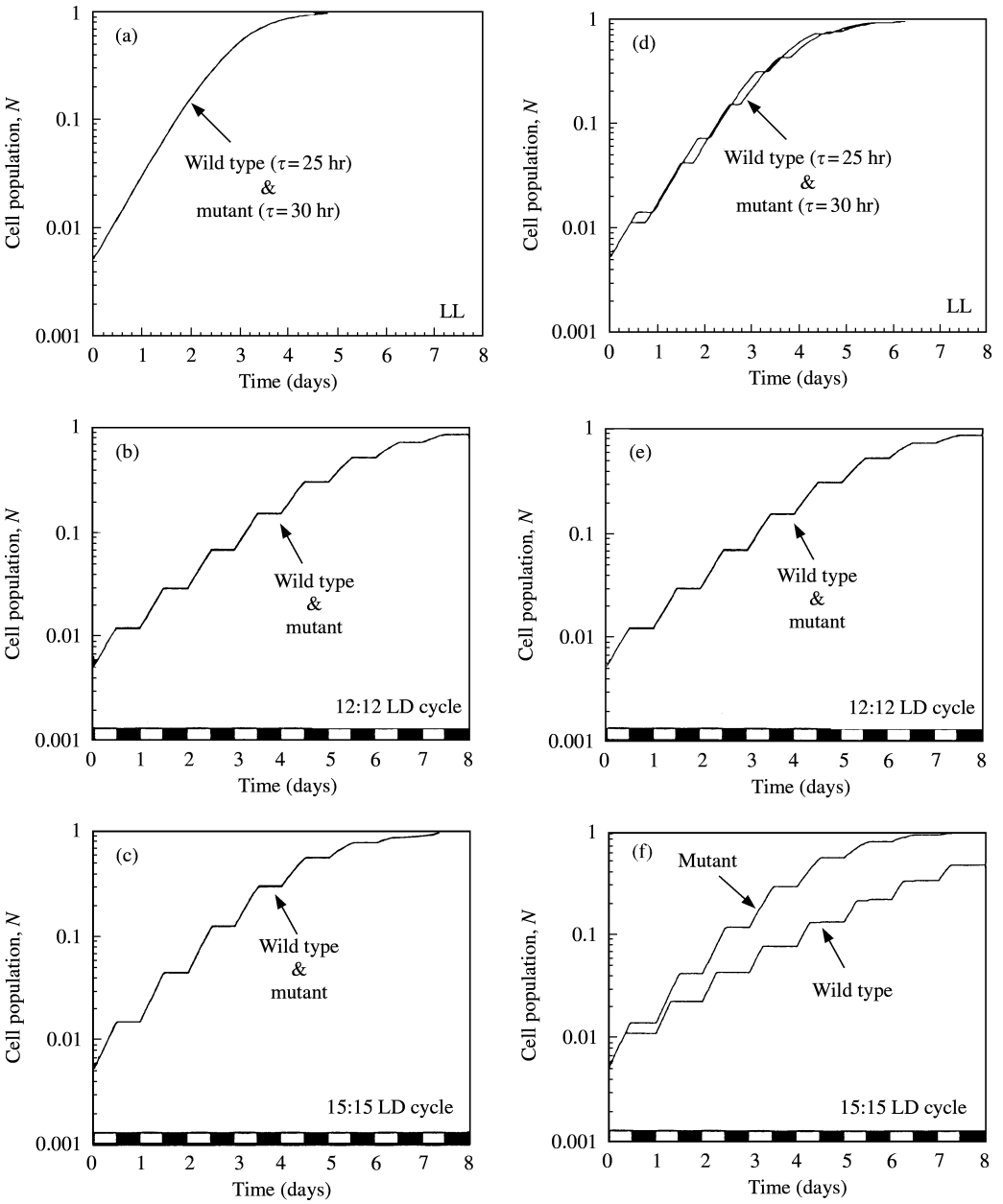

FIG. 5. Growth of individual strains in LL (a), or in a 12:12 LD cycle (b) or 15:15 LD cycle (c). The growth curves pertain to cultures containing the wild-type ($\tau = 25$ hr) or long-period mutant ($\tau = 30$ hr) strains alone. The time evolution of each cell population is determined by numerical integration of eqns (1) subjected to conditions (2) and of eqns (3). Parameter values for panels (a)–(c) (used throughout this study unless otherwise specified) are $k = 1.8$, $I_c = 0.01$, $p = 500$, $V_{max} = 1000$, $K_M = 0.05$; the dilution factor γ is equal to 0 (batch culture). Concentrations are in arbitrary units while time is expressed in days. For these parameter values, the growth curves for the two strains are indistinguishable, as observed in the experiments. At lower values of the maximum rate of inhibitor degradation, e.g. $V_{max} = 300$ [panels (d)–(f)], the model can produce different growth curves for the two strains in some LD cycles [panel (f), illustrating the case of a 15:15 LD cycle] while the two curves remain nearly undistinguishable in a 12:12 LD cycle (e) or in LL (d).

L phase starts, when cells are still in sD because the inhibitor is only secreted during sL and cells have enough time to degrade it during the time separating the onset of sD from the beginning of L. As a consequence, the long-period mutant grows during the entire L phase. In contrast, when the beginning of sD falls in L, as occurs for the wild type, the latter cannot grow after the sL

to sD transition as long as $I > I_c$. Therefore, in monocultures placed in a 30-hr LD cycle, the wild type is disadvantaged when compared to the long-period mutant. As a result, the curve showing the growth of the wild type in Fig. 5(f) is shifted to the right of the curve for the mutant. Such differences are not observed in the experiments, suggesting that the degradation of the inhibitor is rapid enough to obscure growth differences between strains with distinct FRPs, as occurs in the model in the case considered in Fig. 5(b).

In contrast to the situation illustrated in Fig. 5(f), no significant differences between the wild-type and long-period mutant are observed in the model at the lower value of V_{max} considered in Fig. 5(d)–(f) when monocultures are subjected to a 24-hr LD cycle [Fig 5(e)]. Indeed, the two strains then have a negative phase angle, so that just after the sL–sD transition which occurs in D, growth does not occur for either strain, and no significant difference can build up in the course of time.

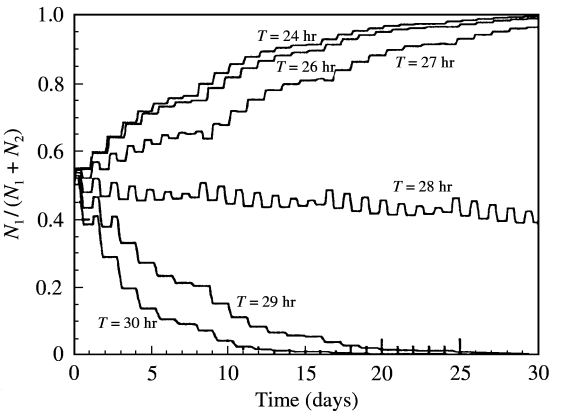

FIG. 6. The outcome of the competition between strain 1 (wild-type, $\tau = 25$ hr) and strain 2 (long-period mutant, $\tau = 30$ hr) depends on the period T of the external LD cycle. The LD cycles are symmetrical, i.e. the L and D phases have similar durations equal to $T/2$. For $T = 24$ to 27 hr, strain 1 dominates strain 2, while the reverse outcome is observed for $T = 29$ or 30 hr. For the intermediate value $T = 28$ hr, a prolonged phase of coexistence between the two strains is predicted. The curves are obtained by numerical integration of eqns (1) subjected to conditions (2) and of eqns (3). The fraction of population 1 in the mixed culture is shown as a function of time. The initial proportions of the two strains in the culture are equal, i.e. $F_1(0) = F_2(0) = 0.5$. The initial values of the two cell populations are $N_1(0) = N_2(0) = 0.005$. Every eight days the culture is diluted (as in the experiments) by dividing variables N_1, N_2 and I by a factor of 100.

3.3. COMPETITION BETWEEN WILD-TYPE AND MUTANT STRAINS IN LD CYCLES OF VARIOUS PERIODS

3.3.1. *Competition Between Two Strains with Different Free-running Periods*

After showing that the growth dynamics of monocultures in LL and LD can be similar despite the differences in FRP, we now turn to the competition of two strains and first investigate the influence of the period of the LD cycle on the outcome of the competition between two strains with different FRPs. In Fig. 6 we simulate the competition between the wild-type ($\tau = 25$ hr) and the long-period mutant ($\tau = 30$ hr) strains denoted by strains 1 and 2, respectively.

The fraction F_i of cells belonging to strain i in a medium containing n different strains is defined by

$$F_i(t) = \frac{N_i(t)}{\sum_{j=1}^{n} N_j(t)}. \qquad (4)$$

We initiate the competition between the wild-type and the long-period mutant with equal fractions of the two strains in the medium, i.e. $F_1(0) = F_2(0) = 0.5$. As shown in Fig. 6, where the fraction of cells from the wild type (strain 1) is represented as a function of time, the outcome of the competition markedly depends on the period T of the LD cycle. At values of T below 28 hr, the wild-type strain overcomes the long-period mutant. The rate at which strain 1 eliminates strain 2 increases as T decreases. When T is larger than 28 hr, strain 2 overcomes strain 1. Here, the larger T is, the quicker strain 2 wipes out strain 1. For $T = 28$ hr the two strains coexist for a long time, but the trend shown in Fig. 6 indicates that strain 2 progressively takes the advantage over strain 1. The small fluctuations in the time evolution of fraction F_1 are due to the asynchrony between the growth phases of the two strains.

The results shown in Fig. 6 agree with the experimental observations of Ouyang *et al.* (1998) which demonstrate a resonance effect. In an LD cycle of given period, the strain that wins the competition is the one whose FRP is closest to the period of the LD cycle. Here, the wild type

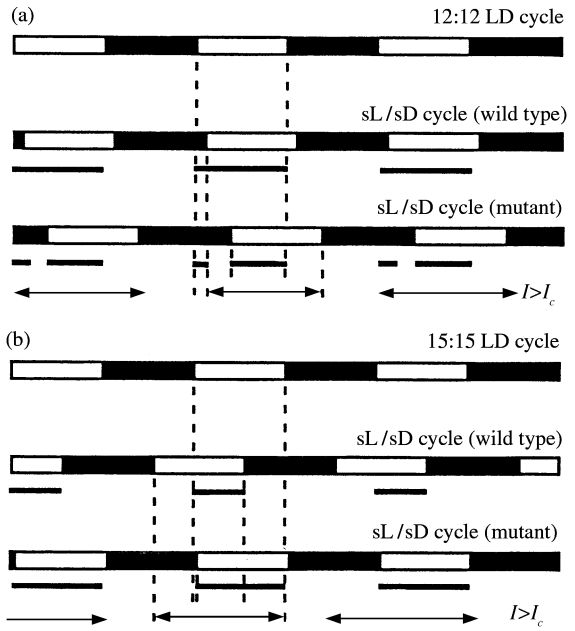

FIG. 7. Schematic explanation of fitness enhancement based on resonating circadian clocks. The panels illustrate the competition between the wild-type ($\tau = 25$ hr) and long-period mutant ($\tau = 30$ hr) strains in a 12:12 LD cycle (a) and a 15:15 LD cycle (b), when equal proportions of the two strains are initially present in the culture. Each panel shows, from top to bottom, the L and D phases of the LD cycle, the sL and sD phases of the wild-type strain, the periods during which this strain grows (solid bar), the sL and sD phases of the long-period mutant and its periods of growth (solid bar), and the periods during which the inhibitor level exceeds the threshold I_c (solid bar with double arrows). The strain that wins the competition in each case is that for which the cumulated growth phase over an LD cycle is longest. Panels (a) and (b) pertain to the competition curves shown in Fig. 6 for $T = 24$ and 30 hr, respectively.

with an FRP of 25 hr outcompetes the long-period mutant with an FRP of 30 hr in LD cycles with a period extending from 24 to 27 hr, while the outcome of the competition is reversed in LD cycles with a period ranging from 28 to 30 hr.

The model allows a detailed exploration of the resonance mechanism by which the circadian clock enhances fitness in cyanobacteria whose FRP most closely matches the period of the LD cycle. In Fig. 7 we examine the cases of a 12:12 LD cycle (panel a) and of a 15:15 LD cycle (panel b) which produce, as shown in Fig. 6, opposite outcomes of the competition between the wild-type and long-period strains. In each panel, from top to bottom, are shown the L and D phases of the LD cycle, the sL and sD phases of the wild-type strain with the underlying solid bar representing periods of growth, the sL and sD phases for the mutant with growth periods similarly represented, and finally, represented by a solid bar with arrows, the periods during which the inhibitor level exceeds the threshold I_c.

In the case of a 12:12 LD cycle, we see that the sL phase of the wild type overlaps better with L than the sL phase of the mutant. As a result, the growth period is longer for the wild type than for the mutant. The wild type begins growing as soon as L begins; indeed, it is then still in sD but the level of inhibitor is below the threshold I_c. It continues to grow until the end of L, and ceases to grow when D begins, even though it is still in sL. Thus, the wild type grows during the entire L phase of the LD cycle. In contrast, the mutant's circadian rhythm is delayed with respect to the LD cycle ($\theta < 0$; see Fig. 4). When L begins, it is still in sD but begins to grow because $I < I_c$. Shortly thereafter, however, the wild type enters sL and begins to secrete the inhibitor. This leads to growth arrest for the mutant. The latter only resumes growth when entering sL, as this occurs in L. Growth of the mutant only occurs during part of sL, because it stops at the end of the L phase which occurs before the end of sL.

The vertical dotted lines in Fig. 7(a) indicate that the growth of the wild type starts at the same time as that of the mutant strain, precisely when L starts. Growth for the two strains also stops at the same time when D begins. The only difference between the two strains is that growth of the wild type spans the whole L phase, whereas growth of the mutant is interrupted between the entrance of the wild type in sL and the beginning of its own sL phase. As a result, the growth period of the mutant is reduced with respect to that of the wild type, and the latter wins the competition.

In the case of a 15:15 LD cycle [Fig. 7(b)], the comparison of the growth periods for the wild-type and mutant strains shows that the latter takes the advantage over the wild type. Indeed, due to the resonance effect, the sL phase of the mutant coincides with L while the sL phase of the wild type is advanced with respect to L ($\theta > 0$; see Fig. 4). The mutant thus grows during nearly the whole of L phase while the wild type only grows during part of the L phase, just after the transition from D to L, until its sD phase begins, during which it is sensitive to the inhibitor secreted by the mutant.

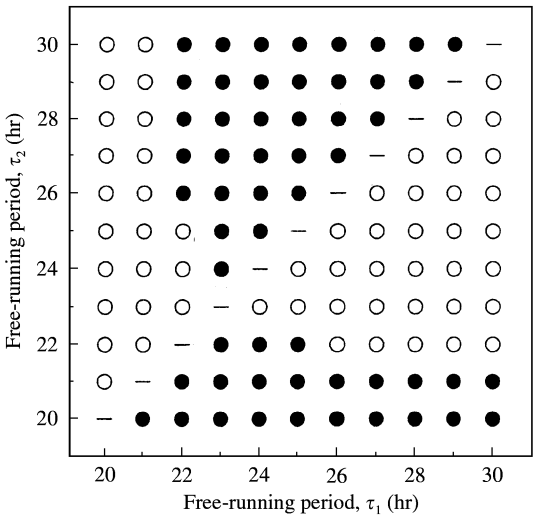

FIG. 8. Outcome of competition between two strains as a function of their free-running periods in a 12:12 LD cycle. The FRPs of strains 1 and 2, denoted by τ_1 and τ_2, range from 20 to 30 hr. A filled circle indicates that strain 1 eventually dominates strain 2, while an empty circle indicates the opposite outcome; a dash denotes coexistence of the two strains. The initial proportions of the two strains in the mixed culture are equal. Numerical simulations are performed as described in the caption to Fig. 6. (●) $F_1 \to 1$, $F_2 \to 0$; (○) $F_1 \to 0$, $F_2 \to 1$; (–) coexistence.

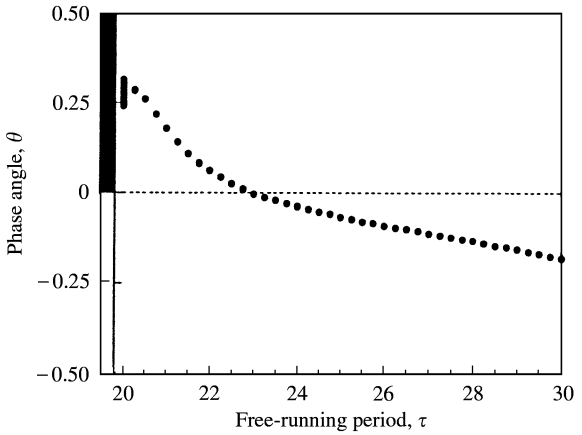

FIG. 9. Dependence of the phase angle θ on the free-running period (τ) of circadian oscillations in a 12:12 LD cycle. The phase angle goes from a positive value (sL advanced with respect to L) to a negative value (sL delayed with respect to L) as τ progressively increases from 20 to 30 hr. At small values of τ, the phase is labile but remains confined in a restricted range of phases. The curve is generated by computer simulations as described in the legend to Fig. 4.

A global picture of the competition between two strains with different FRPs in a 12:12 LD cycle is shown in Fig. 8. There, the FRP of each of the two strains is varied by 1-hr intervals from 20 to 30 hr, and the outcome of the competition is indicated by a filled circle when population 1 (of FRP denoted τ_1) wins, by an empty circle when population 2 (of FRP denoted τ_2) takes over, and by a dash in the case of coexistence of the two populations. At the level of resolution considered, coexistence is only seen when the two strains possess the same FRP. Moreover, the results display an antisymmetry with respect to the bisecting line (the outcome of the competition between two strains 1 and 2 with FRPs equal to 22 and 26 hr is naturally the opposite of that obtained for the competition between strains 1 and 2 with FRPs equal to 26 and 22 hr). Several characteristics of the competition profile in Fig. 8 are worth noting: when population 1 has an FRP of 20 hr, the other population always overcomes the first when $21\text{ hr} < \tau_2 < 30\text{ hr}$. When $\tau_1 = 23\text{ hr}$, the first population always overcomes the second in the interval $20\text{ hr} < \tau_2 < 30\text{ hr}$ except when $\tau_1 = \tau_2$. Particularly interesting is the result that slightly below and above the 24-hr period of the LD cycle, e.g. for $\tau_1 = 22$ and 26 hr there is an intermediate range of τ_2 values for which the second population overcomes the first, while the reverse outcome is observed below and above this range of values of τ_2.

To understand the resonance mechanism leading to the competition results obtained in Fig. 8 for a 12:12 LD cycle, it is useful to determine how the phase angle θ varies with the FRP in such an LD cycle. The data of Fig. 9 indicate that the value of θ decreases from a positive value (advance of sL with respect to L) to a negative value (delay of sL with respect to L) as the FRP (τ) goes from 20 to 30 hr. The phase angle becomes nil (coincidence of sL with L) for a value of τ close to 23 hr. (The fact that perfect concomitance of sL and L occurs for τ close to 23 hr rather than $\tau = 24$ hr is due to the arbitrary way in which we defined sL as the phase during which variable x in the light-entrained van der Pol oscillator is positive.) The comparison of Figs 8 and 9 shows that the strain that wins the competition is roughly the one whose phase angle has the smallest absolute value, i.e. the strain for which the overlap of sL with L is more extended.

3.3.2. *Influence of Initial Conditions on the Outcome of Competition Experiments*

The model indicates that the outcome of competition experiments between two strains is not only dictated by the relative values of the FRPs of the two strains with respect to the period of the LD cycle, but also by the initial fractions of the two strains in the culture. Yet another important factor is the value of the threshold concentration of inhibitor, I_c, above which growth of a strain in sD is inhibited in L. The effect of this parameter will be considered in the next section. For a fixed value of $I_c = 0.01$, we illustrate the effect of the initial fractions of competing strains in the cases of a 12:12 LD cycle [Fig. 10(a)] and of a 15:15 LD cycle [Fig. 10(b)]. In the former case, when the initial fraction $F_1(0)$ of cells of strain 1 is smaller than about 0.4, the two strains coexist. For larger values of $F_1(0)$, strain 1 wins the competition. The larger the initial fraction of strain 1, the faster this strain excludes strain 2.

The situation is different in the case of a 15:15 LD cycle. Then, indeed, strain 2 wins the competition as long as the initial fraction $F_1(0)$ is equal to or smaller than 0.6, while strain 1 overcomes strain 2 when $F_1(0)$ is equal to or larger than 0.7, despite the fact that the FRP of strain 2 is closer to the period of the LD cycle than the FRP of strain 1.

The comparison between Fig. 10(a) and (b) indicates that the progressive increase in the initial fraction of strain 1 leads either to a switch from coexistence to dominance of strain 1 (as seen for a 12:12 LD cycle), or to a switch from dominance of strain 2 to dominance of strain 1 (as observed for the 15:15 LD cycle). These results can be explained according to the relative phase angles of the two strains in the two LD cycles [see also Roussel *et al.* (2000) for a similar explanation based on our previous model]. When the initial fraction of strain 1 decreases in a 12:12 LD cycle [see Fig. 7(a)], the advantage of strain 1 over strain 2 eventually disappears and the two strains coexist, because strain 1 cannot secrete enough inhibitor to contain the growth of strain 2 during the period in sD where such growth was prevented when initial fractions of strains 1 and 2 were equal [as in the case illustrated in Fig. 7(b)]; coexistence occurs because the two strains grow during the whole phase L.

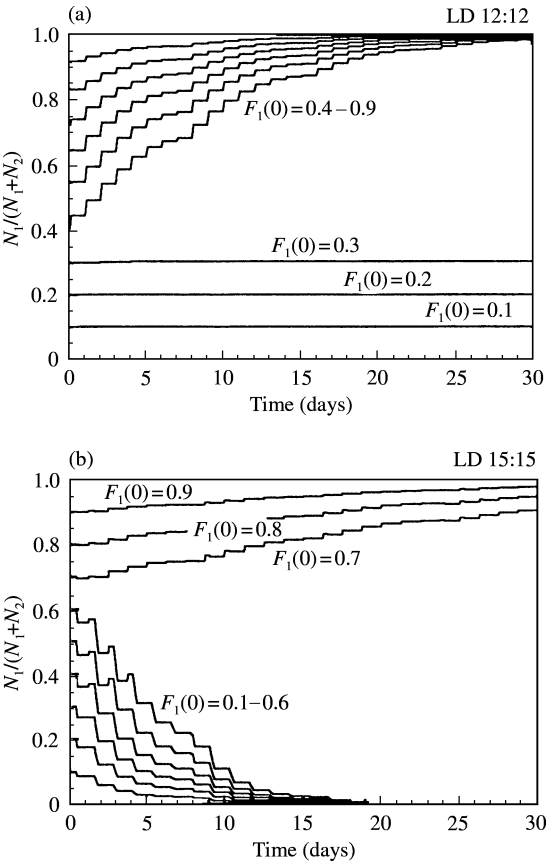

FIG. 10. Outcome of competition between the wild-type ($\tau = 25$ hr) and long-period mutant ($\tau = 30$ hr) strains in a 12:12 LD cycle (a) and a 15:15 LD cycle (b) as a function of the initial fraction $F_1(0)$ of wild-type cells in the mixed culture. In panel (a), strain 1 wins the competition when its initial fraction is equal to or larger than 0.4; below this value the model predicts the coexistence of the two strains. In panel (b), strain 1 wins the competition when its initial fraction is larger than 0.6 while it is eliminated by strain 2 when $F_1(0)$ falls below this value. Simulations are performed as described in the legend to Fig. 6.

In a 15:15 LD cycle, sL of strain 1 is advanced with respect to L, while sL of strain 2 is slightly delayed with respect to L. As a consequence, for equal values of the initial fractions of strains 1 and 2 [Fig. 7(b)], growth of strain 1 is impeded in sD because of the inhibitor secreted by strain 2, which in contrast grows during nearly entire L due to better overlaps with sL. When the initial fraction of strain 2 decreases to sufficiently low levels, the inhibitor secreted by this strain in sL is not capable of preventing the growth of strain 1 in the part of sD overlapping with L. Hence, strain 1 grows during entire L, while strain 2 grows as long as sL overlaps with L, but not

during the brief time when sD overlaps with L, since the inhibitor is then secreted by strain 1 at high concentration. This difference in growth period leads to strain 1 eliminating strain 2 at sufficiently large values of the initial fraction $F_1(0)$.

3.3.3. *Influence of Inhibition Threshold*

To illustrate the effect of the inhibition threshold I_c, we have determined as a function of this threshold the minimum initial fraction of strain 1 required to ensure dominance of this strain over strain 2. In the case of the 12:12 LD cycle, the minimum value of $F_1(0)$ increases with I_c [Fig. 11(a)]. As explained above, the boundary curve in the $F_1(0)$ vs. I_c plane then separates a region of dominance of strain 1 from a region of coexistence between the two strains considered. In the case of a 15:15 LD cycle, the boundary curve has the opposite slope: the minimum value of $F_1(0)$ required for dominance of strain 1 decreases as I_c increases [Fig. 11(b)]. Solid curves in Fig. 11 have been obtained by means of numerical simulations. The dashed lines have been obtained by applying the analytical expression derived in our previous study for the critical initial fraction $F_1(0)$ as a function of I_c. This analytical expression remains valid for the present model. Indeed, it only relies on a discussion of cell growth based on the evolution equation for the inhibitor concentration (see Appendix A in Roussel *et al.*, 2000) and does not depend on the way the circadian oscillator kinetics generates the phase angle θ.

The reason underlying the difference between the two situations considered in Fig. 10 is that in the case illustrated in Fig. 11(a), strain 1 is nearly insensitive to the inhibitor while strain 2 is sensitive to it during part of its sD phase [Fig. 7(a)]; in contrast, in the case illustrated in Fig. 11(b), it is strain 1 that is sensitive to the inhibitor during part of its sD phase, while strain 2 is mostly insensitive to it [Fig. 7(b)]. Therefore, when I_c increases, in the 12:12 LD cycle the inhibitory effect of strain 1 is reduced and more cells of this strain are needed to inhibit the growth of strain 2, while in the 15:15 LD cycle the inhibitory effect of strain 2 diminishes and fewer cells of strain 1 are required initially to ensure the advantage of the latter strain.

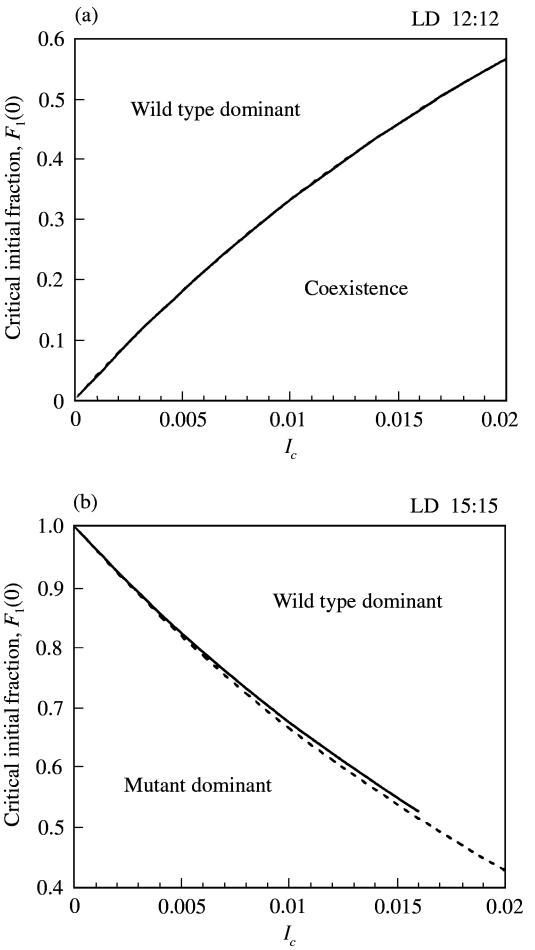

FIG. 11. Outcome of competition between the wild-type (strain 1, $\tau = 25$ hr) and long-period mutant (strain 2, $\tau = 30$ hr) cells in a 12:12 LD cycle (a) and a 15:15 LD cycle (b) as a function of the inhibition threshold I_c. Shown in each panel as a function of I_c is the minimum value of the initial fraction of cells of strain 1 required to ensure dominance of this strain over strain 2. In a 12:12 LD cycle, coexistence between the two strains is observed below the critical curve, while in a 15:15 LD cycle, a switch to dominance of the mutant occurs below the curve. Solid curves, obtained by means of numerical integration of the model equations, yield good agreement with the values (dashed lines) plotted according to the analytical expression derived in our previous study for the critical initial fraction $F_1(0)$ as a function of I_c [eqn (A.3) in Roussel *et al.*, 2000]. The interruption of the solid curve in (b) is due to difficulties in numerical integration.

3.3.4. *Effect of Photoperiod*

So far we have considered only the symmetrical case of LD cycles with equal L and D phases. The natural LD cycle has a photoperiod that varies over the year. Thus, with regard to the physiological aspects of the resonance phenomenon, the question arises as to whether the

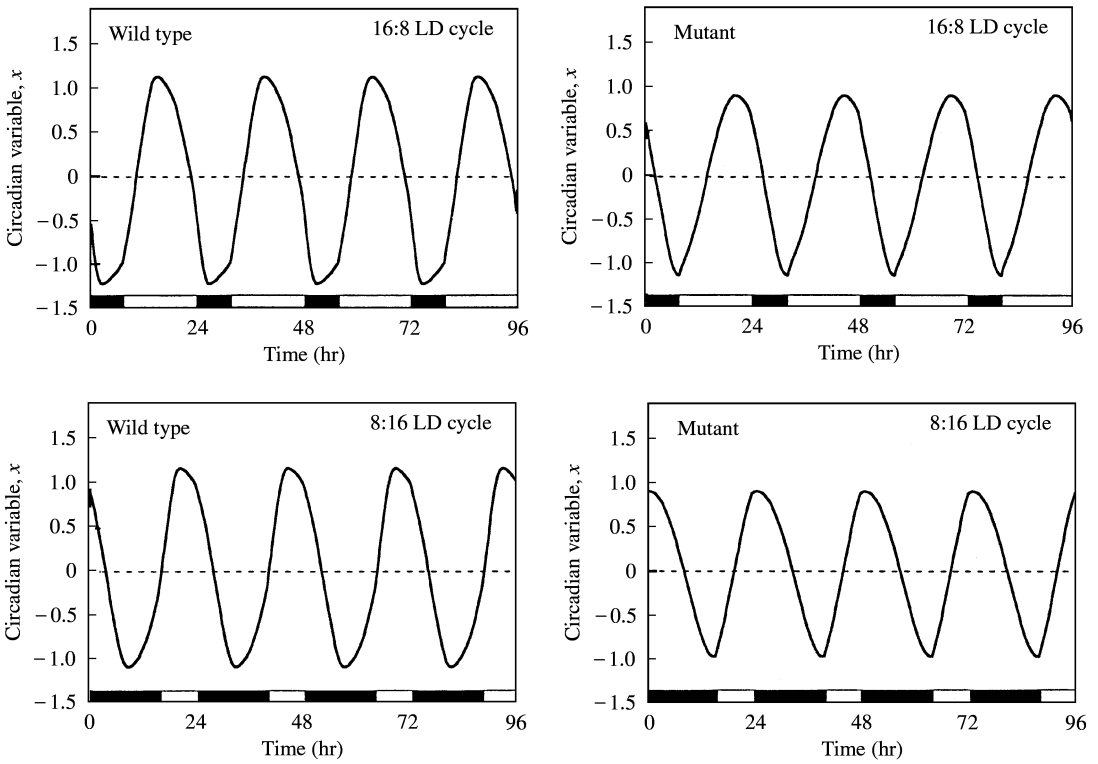

FIG. 12. Effect of photoperiod of LD cycle on entrainment of the circadian oscillator. The circadian oscillations produced by the modified van der Pol model in the wild-type ($\tau = 25$ hr; left column) and the long-period mutant ($\tau = 30$ hr; right column) strains of cyanobacteria entrained by a 16:8 LD cycle (upper row) and a 8:16 LD cycle (bottom row) are shown. The evolution of variable x, determined by the numerical integration of eqns (3), is shown as a function of time. Parameter values are as shown in Fig. 3. The overlap of the sL phase ($x > 0$) with the L phase is better in the wild type than in the long-period mutant. The reverse is true in a 15:15 LD cycle (data not shown).

competition experiments lead to similar outcomes regardless of the relative durations of the L and D phases for a given period of the LD cycle.

We first illustrate in Fig. 12 the effect of the photoperiod for a 24-hr LD cycle by showing that the van der Pol oscillator model can be entrained by a 16:8 and a 8:16 LD cycle both in the cases of the wild type ($\tau = 25$ hr) and of the long-period mutant ($\tau = 30$ hr). The two left panels show that the resonance effect is recovered at the two photoperiods. Indeed, the sL phase corresponding to positive values of variable x has better overlap with L for the wild type as compared to the long-period mutant (right panels). Similarly, in the case of 10:20 and 20:10 LD cycles, the sL phase shows better overlap with L in the long-period mutant compared to the wild type (data not shown).

When the wild-type and long-period mutant strains are subjected to a 8:16 or 16:8 LD cycle, starting with equal fractions of the two strains, the wild type takes the advantage in both cases over the other strain. In contrast, when the same two strains are subjected in similar conditions to a 10:20 or 20:10 LD cycle, the long-period mutant takes over (Fig. 13). These results are similar to those obtained for symmetrical LD cycles (see Fig. 6) and can be explained in the same way. Therefore, the phenomenon of enhanced fitness due to resonating circadian clocks remains robust with respect to the varying photoperiod.

3.4. COMPETITION BETWEEN THREE STRAINS

So far experimental studies of competition in LD cycles of varying period have been performed by mixing two cyanobacterial strains at a time and determining the outcome of the competition between these two strains. It is of interest to investigate how the introduction of a third bacterial strain affects the outcome of competition.

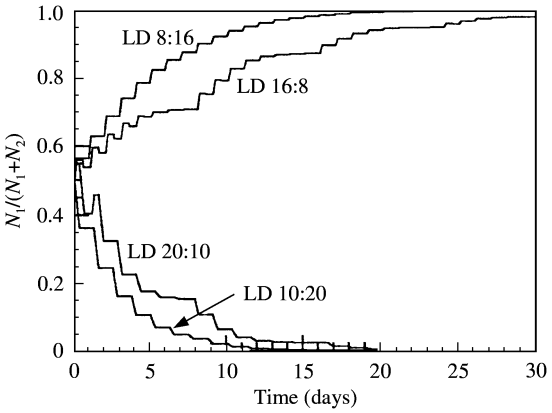

FIG. 13. Effect of photoperiod on the outcome of competition between wild-type (strain 1, $\tau = 25$ hr) and long-period mutant (strain 2, $\tau = 30$ hr) cells in LD cycles of 24 or 30 hr period. Starting from equal proportions of the two strains, strain 1 wins the competition in an 8 : 16 or 16 : 8 LD cycle, while strain 2 dominates strain 1 in a 10 : 20 or 20 : 10 LD cycle. Simulations were performed as described in Fig. 6.

This question can readily be addressed by means of the model. To illustrate the case of such a "compétition à trois" we consider the situation where the wild-type (strain 1, $\tau = 25$ hr) and the long-period (strain 2, $\tau = 30$ hr) strains are mixed with a strain of intermediate period (strain 3, $\tau = 27$ hr).

The results of the competition between the three strains, initially present in equal proportions [$F_1(0) = F_2(0) = F_3(0) = 1/3$] in the case of symmetrical LD cycles of period equal to 24 hr [panel (a)], 30 hr [panel (b)] and 27 hr [panel (c)] are shown in Fig. 14. The model indicates that the resonance phenomenon observed for the competition between two strains also occurs for the competition between three strains, even though all strains possess similar characteristics of individual growth in LL and in LD. The comparison of panels (a)–(c) in Fig. 14 leads to two main conclusions: (i) the strain that wins the competition is generally the one whose FRP is closest to the period T of the LD cycle, i.e. strain 1 for $T = 24$ hr [panel (a)] and strain 2 for $T = 30$ hr [panel (b)]; (ii) the strain that is eliminated first is generally that whose FRP is farthest from T, i.e. strain 2 for $T = 24$ hr, and strain 1 for $T = 30$ hr.

The situation illustrated in panel c of Fig. 14 is somewhat more complex and leads to a less straightforward interpretation. There, in a 27-hr-period LD cycle, the strain that is first eliminated is the one with an FRP of 30 hr, but the strain with an FRP of 27 hr is eventually eliminated by

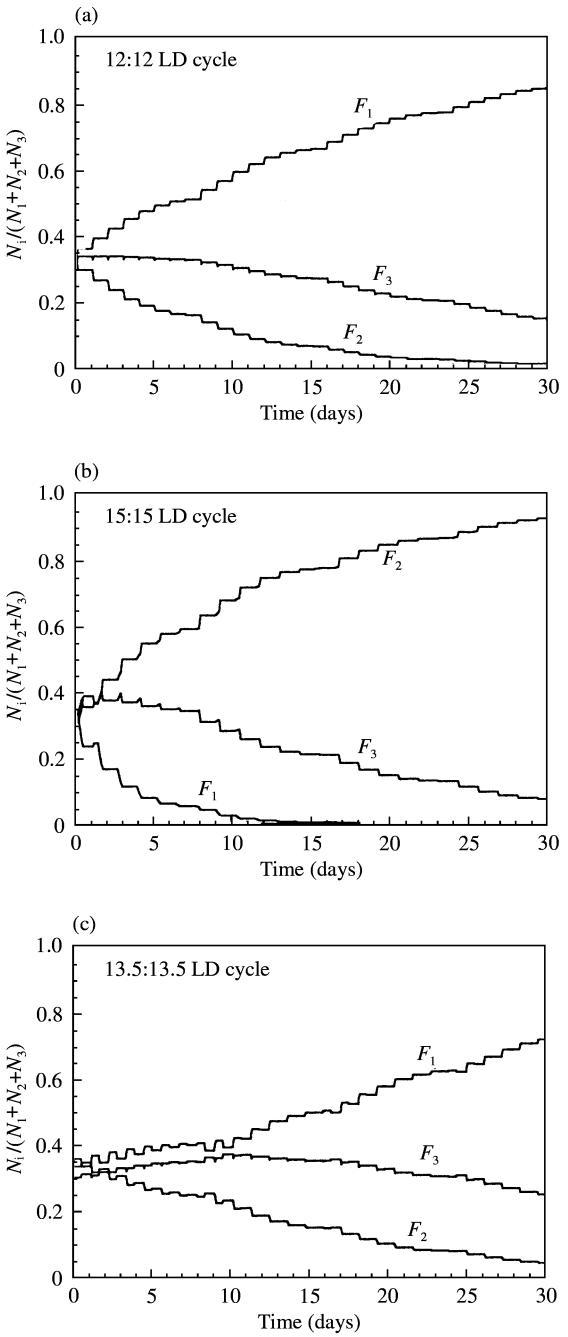

FIG. 14. Competition between three strains. Strains 1 ($\tau = 25$ hr) and 2 ($\tau = 30$ hr) are mixed with a third strain ($\tau = 27$ hr); all three strains are initially present in equal proportions. Strain 1 eliminates the other two strains in a 12 : 12 LD cycle (a), while strain 2 wipes out the other strains in a 15 : 15 LD cycle (b). In a 13.5 : 13.5 LD cycle (c), the situation is less clear-cut, and strain 1 eventually overcomes strains 2 and 3 (see text).

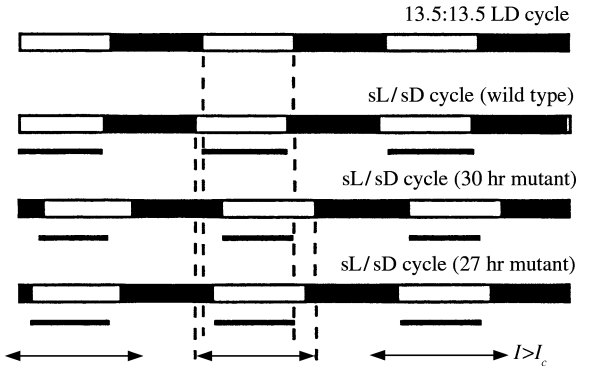

FIG. 15. Schematic explanation of fitness enhancement based on resonating circadian clocks in the case of a competition between three strains placed in a 13.5:13.5 LD cycle. Strains 1 ($\tau = 25$ hr) and 2 ($\tau = 30$ hr) are mixed with a third strain ($\tau = 27$ hr); all three strains are initially present in equal proportions. The results correspond to the time evolution shown in Fig. 14(c). Shown from top to bottom, are the L and D phases of the LD cycle, the sL and sD phases of the wild-type strain, the periods during which this strain grows (solid bar), and corresponding data for strains 2 and 3. The arrowed bar at the bottom indicates the periods during which the inhibitor level exceeds the threshold I_c. Strain 1 wins the competition [see Fig. 14(c)] because its growth phase over an LD cycle is slightly longer than that of strain 3, which itself fares better than strain 2.

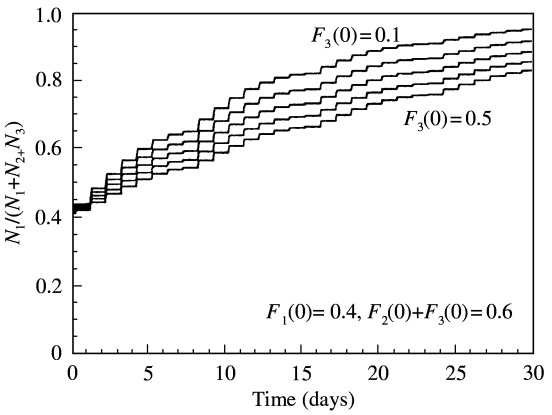

FIG. 16. Effect of initial proportions of the two mutant strains 2 ($\tau = 30$ hr) and 3 ($\tau = 27$ hr) on their competition with the wild-type strain 1 ($\tau = 25$ hr) in a 12:12 LD cycle. Keeping a constant initial fraction $F_1(0)$ equal to 0.4, we vary the initial fractions $F_2(0)$ and $F_3(0)$ while keeping their sum equal to 0.6. The curves show a progressive slowing down of the establishment of strain 1 dominance as the initial proportion of strain 3 increases from 0.1 (top curve) to 0.5 (bottom curve) in the culture. Simulations were performed as described for Fig. 6, by applying eqns (1) to the case of three distinct populations.

the wild-type strain, of 25-hr FRP, even though the latter FRP is further from the period of the LD cycle than the FRP of the eliminated strain 2. As indicated in Fig. 15, this paradoxical result is due to the phase angle relationships of the three strains with respect to the LD cycle. Strain 1 is slightly advanced, and strain 3 is slightly delayed with respect to the LD cycle. Strain 1 begins to grow when L starts, and stops growing when sL ends. Strain 3 begins to grow when sL starts (indeed, as a result of the secretion of inhibitor by strain 1, during sD strain 3 cannot grow because $I > I_c$) and stops growing when L ends. The slightly longer duration of growth of strain 1 ensures its long-term elimination of strain 3. Strain 2, which is more delayed with respect to the LD cycle, is eliminated more rapidly as its growth is more restricted than that of the other two strains (see Fig. 15).

To know whether the elimination of the 27-hr-FRP mutant by the wild type is due to the initial presence of a third strain in the culture, it is of interest to determine the outcome of the competition between the wild type and the mutant in a 27-hr-period LD cycle. The simulations show that starting with equal proportions, for some 100 days the two strains coexist, before the mutant finally overcomes the wild type. The opposite result found in the initial presence of a third strain might suggest that this difference in outcome originates from a three-strain effect. However, the particular case considered appears to represent a rather special case.

Another effect of the presence of a third strain is that it can slow down the takeover of the strain for which the FRP is closest from the period of the LD cycle. In Fig. 16, we consider the same three strains as above, subjected to a 12:12 LD cycle. In these conditions, as shown in Fig. 13(a), strain 1 wins the competition. We start with the same initial fraction, equal to 0.4, and vary the proportions of strains 2 and 3 in such a way that the sum of their initial fractions remains equal to 0.6. As shown in Fig. 16, the takeover of strain 1 becomes progressively slower as the initial fraction of strain 3 increases. Such a slowing down is due to the fact that strain 3 is a better competitor of strain than strain 2 in a 24-hr LD cycle because the FRP of strain 3 is closer to 24 hr.

4. Discussion

A clear-cut experimental demonstration of the fitness-enhancing role of circadian rhythms has

recently been presented for cyanobacteria (Ouyang *et al*., 1998). Observations performed in light–dark cycles of various periods have indeed shown that the selection of cyanobacterial strains markedly depends on the period of their endogenous circadian oscillations. When starting with mixtures of two strains of different free-running period, the strain that is selected is generally that which has an FRP closest to the period of the imposed LD cycle. This resonance phenomenon provides a basis for the physiological role of circadian rhythms which allow living organisms to adapt to the natural periodicity of their environment.

In a previous publication, we have proposed a theoretical analysis of the fitness enhancement in cyanobacteria based on resonating circadian clocks (Roussel *et al*., 2000). Our analysis relied on the observation that the phase angle of the circadian cellular oscillator with respect to the LD cycle varies according to the FRP of the cyanobacteria strain. Taking this phase angle as an arbitrarily set parameter, we compared two plausible mechanisms for fitness enhancement based on circadian rhythms in competing strains of cyanobacterial characterized by different free-running periods. The first mechanism relies on competition via secretion of an inhibitor of cell growth; the second mechanism involves the competition for a limiting substrate. The comparison of the two models indicated that the former mechanism can account, better than the latter, for a large set of experimental observations. The existence of a growth inhibitor has already been demonstrated in some species of cyanobacteria (Yamada *et al*., 1993), and the light-dependent character of the secretion of such an inhibitor has been observed in other light-dependent organisms such as *Gonyaulax* (Roenneberg *et al*., 1991).

To explore in further detail the resonance mechanism by which circadian rhythms enhance fitness in cyanobacteria, we have considered here a model in which the phase angle of a given cyanobacterial species with respect to the LD cycle is not imposed *a priori* but is rather generated by the model itself. To this end, we have incorporated an explicit circadian oscillator with control by light, so that the dependence of the phase angle of this cellular oscillator with respect to the LD cycle is generated automatically by the model for each cyanobacterial strain according to its FRP and to the period of the forcing LD cycle.

The molecular mechanism of circadian rhythms in cyanobacteria is still unclear even though a number of clock genes belonging to the *kai* family have already been identified (Ishiura *et al*., 1998). Therefore, rather than resorting to a molecular model for circadian rhythms proposed for other organisms such as *Drosophila* or *Neurospora* for which the molecular mechanism is known in greater detail, we have considered a more abstract model, the van der Pol oscillator, which has long been used to account for key properties of circadian rhythms in a variety of organisms. In the absence of sufficient detailed information on the molecular mechanism of circadian rhythms in cyanobacteria, the use of the van der Pol oscillator allows us to focus on the qualitative aspects of the resonance phenomenon and to study it on a more general level, independent of molecular details.

We started by showing that the modified version of the van der Pol oscillator used in our study (Jewett & Kronauer, 1998; Jewett *et al*., 1999) accounts for free-running oscillations in LL and for entrainment of the oscillations by LD cycles of various periods (Fig. 3). In Fig. 3, as in most subsequent figures, for illustrative purposes we focused primarily on the case of the wild-type and of a long-period strain, characterized by an FRP (τ) of 25 and 30 hr, respectively. We then showed in Fig. 4 how the phase angle of the wild-type and mutant strains varies with the period of the LD cycle.

In addition to the van der Pol oscillator describing the circadian oscillator of cyanobacteria, the model contains a kinetic equation describing the growth of each cyanobacterial strain present in the culture, as well as a kinetic equation describing the secretion and degradation of the growth inhibitor produced by the cells present in the medium. As summarized in Fig. 2, the growth of cells, the secretion of inhibitor and the cell sensitivity toward the inhibitor are assumed to depend on the phase of the LD cycle and on the phase of the internal circadian oscillator. We confirmed the robustness of the results with respect to the precise form of these assumptions by testing the effect of some changes in underlying hypotheses.

As shown in Fig. 5(a) and (b), the model can account for the observation that the wild-type and long-period mutant strains have identical growth curves when cultured alone in the medium, both in LL and in LD, even though one of the two strains can eliminate the other in competition experiments. However, the model indicates that the two strains may possess different growth curves, particularly in LD, at low values of the maximum inhibitor degradation rate, even when the growth parameters of the two strains are the same [Fig. 5(d)].

The resonance phenomenon is illustrated by the simulated competition experiments shown in Fig. 6. As observed in the experiments of Ouyang *et al.* (1998), when starting with equal proportions of the wild-type and long-period mutant strains, the outcome of the competition depends on the period T of the LD cycle: the wild type ($\tau = 25$ hr) outcompetes the mutant ($\tau = 30$ hr) when T ranges from 24 to 27 hr, while the reverse competition outcome is observed when T equals 29 or 30 hr; the case where T is equal to 28 hr leads to a less clear-cut outcome. Based on the difference of phase angle (Fig. 4), the model allows a precise explanation of these results in terms of the relative positions of the sL and sD phases of circadian oscillations within each of the two strains with respect to the LD cycle: of key importance are the differences in the duration of growth phase of each strain, due to the timing of secretion of inhibitor by the other strain and of sensitivity toward this inhibition (Fig. 7).

We generalized the results of competition experiments by showing in Fig. 8, for the case of a 24-hr LD cycle, which one of two strains outcompetes the other when the FRP of each strain varies from 20 to 30 hr. Even though equal proportions of the two strains are present initially in the medium, one strain eventually eliminates the other, except when they have the same FRP. The outcome of the competition depends on the relative values of the two FRPs with respect to the period of the LD cycle. This is strikingly demonstrated by fixing the value of the FRP of one strain and varying the FRP of the other strain from 20 to 30 hr. Then, indeed, the outcome of the competition may change successively as the second FRP increases. Thus, when setting the FRP of strain 1 (τ_1) equal to 26 hr, the model predicts that strain 2 eliminates strain 1 when $\tau_2 = 20$ to 21 hr, while strain 2 is eliminated by strain 1 when τ_2 ranges from 22 to 25 hr. The two strains coexist when $\tau_1 = \tau_2 = 26$ hr. For values of τ_2 larger than or equal to 27 hr, strain 1 again outcompetes strain 2.

The model allowed us to study in detail the influence exerted on the outcome by other factors such as the initial proportions of competing strains and the threshold concentration of inhibitor, I_c, above which the growth of a strain in sD and L is inhibited. In a 12:12 LD cycle, the wild type overcomes the long-period mutant as long as its initial fraction in the medium exceeds 0.4; below this value, the two strains coexist [Fig. 10(a)]. At different forcing periods, a critical value of the initial proportions of the two strains may lead to a switch in the strain that wins the competition. Thus, in a 15:15 LD cycle, the long-period mutant overcomes the wild type as long as the initial fraction of the latter is below or equal to 0.6; however, when its initial fraction is larger, the wild type outcompetes the mutant [Fig. 10(b)]. These results are generalized by plotting as a function of the threshold inhibitor concentration I_c the critical value of the initial fraction of wild-type strain in the medium separating the domains of wild-type dominance and coexistence in a 12:12 LD cycle [Fig. 11(a)], and the domains of dominance of the wild-type and of the long-period mutant in a 15:15 LD cycle [Fig. 11(b)]. The results indicate that the critical fraction above which the wild type dominates the long-period mutant increases with I_c in a 12:12 LD cycle and decreases with I_c in a 15:15 LD cycle.

The above results have been obtained in the symmetrical case where the L and D phases of the imposed LD cycle have equal durations. Extension of the analysis to unequal durations of the L and D phases shows that similar results on fitness enhancement based on resonance of the circadian oscillator with the external LD cycle are recovered regardless of the photoperiod. Thus, results obtained in an 8:16 or 16:8 LD cycle, or in a 10:20 or 20:10 LD cycle, are comparable to those obtained in a 12:12 or 15:15 LD cycle, respectively. The phase angle of the circadian oscillator still varies with the period T of the LD cycle in a manner specific to the FRP

and similar to that observed in Fig. 4 for symmetrical LD cycles. The value of T at which the phase angle θ vanishes depends on the photoperiod and on the value of the FRP (data not shown). The competition kinetics predicted by the model for LD cycles of unequal L and D phases (Fig. 13) is qualitatively unchanged with respect to the kinetics observed for symmetrical LD cycles (Fig. 6); the only noticeable effect of the photoperiod is to alter the speed at which one strain eliminates the other at a given value of period T.

All competition experiments so far have involved only two cyanobacterial strains. The model can be used to predict the outcome of competition between three strains differing by their free-running period. We have shown that the results obtained for two competing strains can be extended to the case where three different cyanobacterial strains are present in the medium. The outcome of the competition again depends on the relative values of the FRPs and of the period of the LD cycle (Figs 14 and 15), as well as on the initial proportions of the three strains. The presence of a third strain merely affects the speed at which another strain is eventually selected (Fig. 16).

Our theoretical examination of the competition between different cyanobacterial strains as a function of the period of the LD cycle was based, for definiteness, on a particular set of assumptions (see Fig. 2). We have verified that similar results are obtained when using slightly different hypotheses. Thus, for example, the resonance effect is recovered when assuming that the inhibitor is secreted by a certain strain only when cells of this strain are in sL and in L (in the above analysis, we assumed that the inhibitor is secreted by cells in sL, regardless of the phase of the LD cycle).

Together with our previous analysis (Roussel *et al.*, 2000), the present results provide a plausible, detailed (though not fully molecular) mechanistic explanation for the experimental observations that demonstrate fitness enhancement in cyanobacteria based on resonating circadian clocks. By explicitly incorporating a sustained cellular circadian oscillator into the model for cell growth, we showed that the experimental results can be accounted for when taking into account (i) secretion of a growth inhibitor by cells at a given phase of their circadian oscillator, (ii) growth during the L phase of the LD cycle when cells are in sL or when they are in sD and the inhibitor is below a critical concentration, and above all (iii) the existence of a phase angle between the circadian oscillator and the LD cycle that is specific to a given cyanobacterial strain and is dictated by the free-running period of the circadian oscillator. Fitness enhancement based on resonance between the circadian oscillator and the LD cycle results from the better superposition of the sL phase of a given cyanobacterial strain with the L phase in a given LD cycle.

Beyond the case of cyanobacteria, the present analysis of fitness enhancement based on resonating circadian clocks provides a theoretical framework for assessing the physiological and evolutionary roles of circadian rhythms in other unicellular or multicellular organisms. The analysis could also extend to the competition between different, normal or pathological cell types subjected to a periodically varying environment or to periodic drug delivery.

This work was supported by grant 3.4607.99 from the *Fonds de la Recherche Scientifique Médicale* (FRSM, Belgium) and by the programme "*Actions de Recherche Concertée*" (ARC 94-99/180) launched by the Division of Scientific Research, Ministry of Science and Education, French Community of Belgium. We thank Dr Carl Johnson for fruitful discussions.

REFERENCES

ALLEMAND, R., COHET, Y. & DAVID, J. (1973). Increase in the longevity of adult *Drosophila melanogaster* kept in permanent darkness. *Exp. Gerontol.* **8,** 279–283.

DUNLAP, J. C. (1999). Molecular bases for circadian clocks. *Cell* **96,** 271–290.

EDMUNDS, L. N. (1988). *Cellular and Molecular Bases of Biological Clocks.* New York: Springer.

GOLDEN, S. S., JOHNSON, C. H. & KONDO, T. (1998). The cyanobacterial circadian system: a clock apart. *Curr. Opin. Microbiol.* **1,** 699–673.

GONZE, D., LELOUP, J.-C. & GOLDBETER, A. (2000). Theoretical models for circadian rhythms in *Neurospora* and *Drosophila*. *C R Acad. Sci.* (*Paris*), *Sér. III* **323,** 57–67.

HUANG, T.-C., TU, J., CHOW, T.-J. & CHEN, T.-H. (1990). Circadian rhythm of the prokaryote *Synechococcus* sp. RF-1. *Plant. Physiol.* **92,** 531–533.

ISHIURA, M., KUTSUNA, S., AOKI, S., IWASAKI, H., ANDERSSON, C. R., TANABE, A., GOLDEN, S. S., JOHNSON, C. H. & KONDO, T. (1998). Expression of a gene cluster *kaiABC* as a circadian feedback process in cyanobacteria. *Science* **281,** 1519–1523.

JEWETT, M. E. & KRONAUER, R. E. (1998). Refinement of a limit cycle oscillator model of the effects of light in the circadian pacemaker. *J. theor. Biol.* **192,** 455–465.

JEWETT, M. E., FORGER, D. B. & KRONAUER, R. E. (1999). Revised limit cycle oscillator model of human circadian pacemaker. *J. Biol. Rhythms* **14,** 493–499.

JOHNSON, C. H., GOLDEN, S. S., ISHIURA, M. & KONDO, T. (1996). Circadian clocks in prokaryotes. *Mol. Microbiol.* **21,** 5–11.

JOHNSON, C. H., GOLDEN, S. S. & KONDO, T. (1998). Adaptive significance of circadian programs in cyanobacteria. *Trends Microbiol.* **6,** 407–410.

KLARSFELD, A. & ROUYER, F. (1998). Effects of circadian mutations and LD periodicity on the life span of *Drosophila melanogaster*. *J. Biol. Rhythms* **13,** 471–478.

KONDO, T. & ISHIURA, M. (1999). The circadian clocks of plants and cyanobacteria. *Trends Plant. Sci.* **4,** 171–176.

KONDO, T., STRAYER, C. A., KULKARNI, R. D., TAYLOR, W., ISHIURA, M., GOLDEN, S. S. & JOHNSON, C. H. (1993). Circadian rhythms in prokaryotes: luciferase as a reporter of circadian gene expression in cyanobacteria. *Proc. Natl Acad. Sci. U.S.A* **90,** 5672–5676.

KONDO, T., TSINOREMAS, N. F., GOLDEN, S. S., JOHNSON, C. H., KUTSUNA, S. & ISHIURA, M. (1994). Circadian clock mutants of cyanobacteria. *Science* **266,** 1233–1236.

KRONAUER, R. E., JEWETT, M. E. & CZEISLER, C. A. (1997). Modeling human circadian phase and amplitude resetting. In: *Biological Clocks*: *mechanisms and applications* (Touitou, Y., ed.) pp. 63–72. Amsterdam: Elsevier.

LELOUP, J.-C. & GOLDBETER, A. (1998). A model for circadian rhythms in *Drosophila* incorporating the formation of a complex between the PER and TIM proteins. *J. Biol. Rhythms* **13,** 70–87.

LELOUP, J.-C. & GOLDBETER, A. (2000). Modeling the molecular regulatory mechanism of circadian rhythms in *Drosophila*. *BioEssays* **22,** 84–93.

LELOUP, J.-C., GONZE, D. & GOLDBETER, A. (1999). Limit cycle models for circadian rhythms based on transcriptional regulation in *Drosophila* and *Neurospora*. *J. Biol. Rhythms* **14,** 433–448.

LIU, Y., TSINOREMAS, N. F., JOHNSON, C. H., LEBEDEVA, N. V., GOLDEN, S. S., ISHIURA, M. & KONDO, T. (1995). Circadian orchestration of gene expression in cyanobacteria. *Genes Dev.* **9,** 1469–1478.

MORI, T., BINDER, B. & JOHNSON, C. H. (1996). Circadian gating of cell division in cyanobacteria growing with average doubling times of less than 24 hours. *Proc. Natl Acad. Sci. U.S.A.* **93,** 10 183–10 188.

OUYANG, Y., ANDERSSON, C. R., KONDO, T., GOLDEN, S. S. & JOHNSON, C. H. (1998). Resonating circadian clocks enhance fitness in cyanobacteria. *Proc. Natl Acad. Sci. U.S.A.* **95,** 8660–8664.

PITTENDRIGH, C. S. & MINIS, D. H. (1972). Circadian systems: longevity as a function of circadian resonance in *Drosophila melanogaster*. *Proc. Natl Acad. Sci. U.S.A.* **69,** 1537–1539.

ROENNEBERG, T., NAKAMURA, H., CRANMER, L. D., RYAN, K., KISHI, Y. & HASTINGS, J. W. (1991). Gonyauline: a novel endogeneous substance shortening the period of the circadian clock of a unicellular alga. *Experientia* **47,** 103–106.

ROUSSEL, M. R., GONZE, D. & GOLDBETER, A. (2000). Modeling the differential fitness of cyanobacterial strains whose circadian oscillators have different free-running periods: comparing the mutual inhibition and substrate depletion hypotheses. *J. theor. Biol.* **205,** 321–340.

SHEEBA, V., SHARMA, V. K., SHUBHA, K., CHANDRASHEKARAN, M. K. & JOSHI, A. (2000). The effect of different light regimes on adult life span in Drosophila melanogaster is partly mediated through reproductive output. *J. Biol. Rhythms* **15,** 380–392.

YAMADA, N., MURAKAMI, N., MORIMOTO, T. & SAKAKIBARA, J. (1993). Auto-growth inhibitory substance from the fresh-water cyanobacterium Phormidium tenue. *Chem. Pharm. Bull.* **41,** 1863–1865.

WILSBACHER, L. D. & TAKAHASHI, J. S. (1998). Circadian rhythms: molecular basis of the clock. *Curr. Opin. Genet. Dev.* **8,** 595–602.